The Dioxygen Adducts of Several Manganese(II) Porphyrins. Electron Paramagnetic Resonance Studies

Brian M. Hoffman,* Thomas Szymanski, Theodore G. Brown, and Fred Basolo

Contribution from the Department of Chemistry and Materials Research Center, Northwestern University, Evanston, Illinois 60201. *Received May 8, 1978*

Abstract: The reversible dioxygen adduct of manganese porphyrin (Mn(Por)) is five coordinate and of intermediate spin state ($S = 3/2$) unlike the adducts of cobalt, iron, and chromium porphyrins. We have prepared a series of Mn(Por)(O_2) complexes, where Por = para-substituted tetraphenylporphyrin ([T(*p*-X)PP]; X = F, H, *n*-BuO) or octaethylporphyrin (OEP), and have examined their magnetic properties. The EPR parameters of the four complexes are qualitatively similar, but do differ within narrow limits: $-D \sim 2\text{-}3.2\ cm^{-1}$; $E/D \sim 1/3$; $-A(^{55}Mn) \sim 52\text{-}54 \times 10^{-4}\ cm^{-1}$; $-B(^{55}Mn) \sim 86\text{-}88 \times 10^{-4}\ cm^{-1}$. We have also remeasured the effects of ^{17}O substitution, and at low temperature (~10 K) find that it is possible to obtain the value of the small ^{17}O hfs constant: $a(^{17}O) \sim 2.3 \times 10^{-4}\ cm^{-1}$. Solely on the basis of the magnetic resonance parameters obtained, it is possible to rule out most possible combinations of an odd-electron configuration and Mn-O_2 binding geometry. These results and qualitative bonding considerations support the original description in terms of a Mn^{IV}-O_2^{2-} valency formalism with a symmetric, edge-on dioxygen.

Our recent EPR studies[1] have shown that the reversible dioxygen adduct of a manganese porphyrin (Mn(Por)) differs appreciably from those of cobalt,[2] iron,[2] and also chromium porphyrins.[3] A primary difference inferred from these measurements is that the Mn(Por) dioxygen adduct is five coordinate (counting O_2 as a single ligand) and not six coordinate as with the others. This conclusion has recently been confirmed in quantitative measurements of the binding of pyridine to Mn(TPP) and of O_2 to Mn(TPP)(py).[4] Second, Mn(Por)(O_2) is of intermediate spin, with three unpaired electrons ($S = 3/2$) and an unusually large zero-field splitting, not low spin as with Fe and Co (but not Cr). Third, the ^{55}Mn hyperfine splittings (hfs) are unusual in their strong anisotropy, and no changes in the EPR spectrum occurred with the use of ^{17}O-enriched O_2, in contrast to the large ^{17}O hfs observed in the Co(Por) dioxygen adducts.[5] A detailed analysis of the EPR results led us to suggest a bonding scheme with three odd electrons on manganese, corresponding to a "^{4}Mn(IV)-peroxo" valency formalism; analogy to other peroxo complexes further suggested a symmetrical, "side-on" geometry.

The task of ascertaining the electronic structure of a Mn(Por)(O_2) from the magnetic resonance data is, however, not straightforward because of the many electronic configurations which might possibly be associated with such a spin-quartet adduct. We have thus prepared several new Mn(Por)(O_2) complexes, where Por = para-substituted tetraphenylporphyrins [T(*p*-X)PP] and octaethylporphyrin (OEP), and have examined their magnetic properties. We have also remeasured the effects of ^{17}O substitution, and at low temperature find that it is possible to actually obtain the value of the small ^{17}O hfs constant. We use the collected magnetic resonance data to reexamine the possible odd-electron configurations of Mn(Por)(O_2), and find that it is possible to rule out most possible combinations of configuration and Mn-O_2 bonding geometry. In particular, our experiments allow us to again dismiss with certainty configurations which have an unpaired electron in the π^* orbital of dioxygen, such as were favored in a recent limited basis set LCAO-MO-SCF calculation.[6] They also support the original suggestion[1] of a formal valency of $Mn^{IV}(O_2^{2-})$ with symmetrically bonded dioxygen.

Experimental Section

All solvents used in the study were reagent grade and used as supplied except where noted. Benzaldehyde, *p*-fluorobenzaldehyde, and pyrrole (Aldrich Chemical) and *p*-*n*-butoxybenzaldehyde (Eastman) were distilled immediately prior to use. Octaethylporphyrin (Strem), $NaBH_4$, and $Mn(C_2H_3O_2)_2 \cdot 4H_2O$ (Alfa Ventron) were used without further purification.

The toluene used for the EPR experiments was purified by refluxing over sodium benzophenone and distilling. It was stored over freshly prepared sodium wire in a vessel equipped with a high-vacuum Teflon valve and an o-ring joint and degassed by a minimum of five freeze-pump-thaw cycles. The ^{17}O-enriched O_2 was obtained from Miles Laboratories, Elkhart, Ind. Anal. ^{17}O, 54.10; ^{18}O, 0.70. Matheson extra dry oxygen was used as obtained. All manipulations of the air-sensitive manganese(II) compounds were performed in Schlenkware[7] using Matheson prepurified N_2 that was further purified by passage through activated Ridox catalyst (Fisher Scientific).

Preparation of the Porphyrins. The tetraarylporphyrins $TPPH_2$, $[T(p\text{-}n\text{-BuO})PP]H_2$, and $[T(p\text{-F})PP]H_2$ were prepared by Adler's method[8] and made chlorin free by Smith's procedure.[9] They were characterized by their visible spectra in benzene.[10]

Preparation of the Porphyrin Manganese(III) Chlorides. All of the Mn(Por)Cl complexes were prepared by the same procedure. The preparation of Mn(TPP)Cl is given in detail as an example.[4b] Manganese was inserted into the porphyrin by adding excess $Mn(C_2H_3O_2)_2 \cdot 4H_2O$ (5.0 g) to $TPPH_2$ (5.0 g) dissolved in 1 L of gently refluxing DMF with no precautions taken to exclude air or light. After refluxing for 30 min an aliquot (ca. 0.1 mL) was withdrawn from the reaction mixture and diluted with ethanol and the completeness of insertion was judged by visible spectroscopy[11] or by the absence of red fluorescence under long-wavelength ultraviolet light.[12] In the unlikely event that conversion was not complete, an additional 250 mg of $Mn(C_2H_3O_2)_2 \cdot 4H_2O$ was added and refluxing continued for 30 min. This process was repeated until no $TPPH_2$ remained. The solution was then poured into 1 L of ice-cold saturated NaCl and cooled to ca. 20 °C in an ice bath. The greenish brown crystalline product was isolated on a medium porosity sintered-disk suction filter and washed with 2 L of water. The moist filter cake was then dissolved in ca. 1200 mL of 50 °C methanol and filtered through the filter from which it came. To this filtrate 250 mL of HCl (concentrated) was cautiously added with swirling. Warm, ca. 50 °C, water was then added until crystallization occurred. This usually required 0.7-1 L depending upon the concentration and temperature of the solutions. After cooling to room temperature, the product, Mn(TPP)Cl, was collected on a suction filter and washed with 1 L of water. After drying overnight (100 °C, 0.1 Torr) 5.22 g of Mn(TPP)Cl was obtained. This material was further purified in 2.00-g lots by crystallization from warm benzene–heptane (1:5 v/v) and dried overnight (100 °C, 0.1 Torr) to yield 1.81 g of pure Mn(TPP)Cl. The Mn(Por)Cl complexes were characterized by their visible spectra[11,13] and contained no EPR-detectable impurities.

Preparation of the Pyridineporphyrinatomanganese(II) Compounds. The procedure of Kobayashi and Yanagawa[14] was used to prepare the Mn(Por)py complexes. Since Mn(OEP)py is quite soluble in methanol, it was crystallized by the addition of N_2-saturated water. The complexes were characterized by their visible spectra in pyridine[4] and by their EPR spectra in toluene, and gave satisfactory elemental analyses.

0002-7863/78/1500-7253$01.00/0

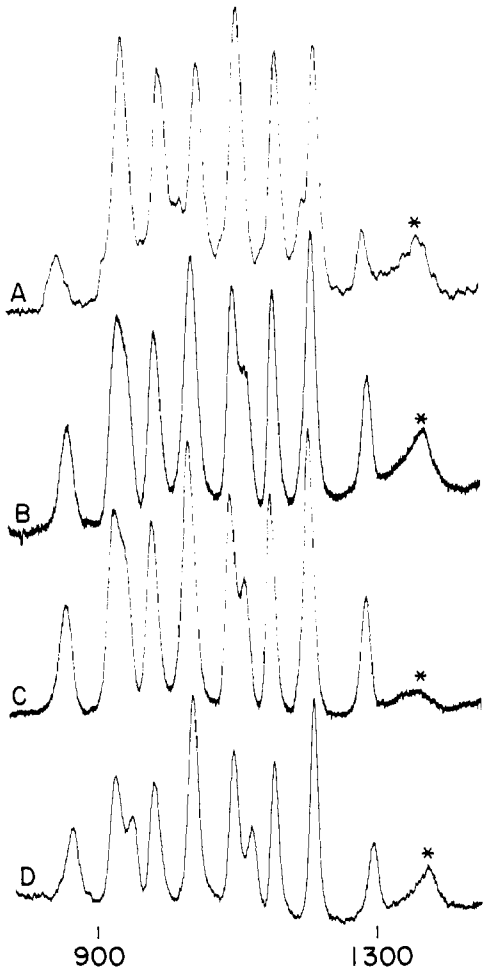

Figure 1. EPR spectra (g = 5.4 region) for (A) Mn(OEP)(O_2); (B) Mn(TPP)(O_2); (C) Mn[T(p-F)PP](O_2); (D) Mn[T(p-n-BuO)PP](O_2); T = 10 K. The concentrations are not the same for the four samples. Spectra are arranged with λ decreasing from spectrum A through D. Magnetic fields are noted in gauss. Asterisk indicates signal from rhombic iron in quartz. $\nu_{microwave}$ = 8.941 GHz.

Preparation of EPR Samples. All EPR spectra were obtained in quartz tubes equipped with high-vacuum Teflon valves and o-ring joints. Samples for the EPR experiments were prepared by two methods: (A) using Mn(Por)py, or (B) using Mn(Por).[4]

Method A. When preparing samples using Mn(Por)py, it is *very* important that the solutions be very dilute since concentrated solutions are extremely difficult, if not impossible, to oxygenate completely. This is caused by the smaller extent of the dissociation described by the reaction Mn(P)py ⇌ Mn(P) + py (K_b), in concentrated solutions at low temperatures.[4] In a typical experiment ca. 0.3 mg of Mn(Por)py was added under a N_2 blanket to a N_2-filled EPR tube. The tube was then attached to a high-vacuum line and evacuated to less than 1 mTorr and ca. 0.5 mL of fully degassed toluene was condensed on the sample by trap to trap distillation.

Method B. Method B is identical with that used for method A except that more (ca. 1 mg) Mn(Por)py was used and the coordinated pyridine was removed by heating the sample in the EPR tube to 250–260 °C for 1 h under dynamic vacuum[4] prior to the addition of solvent. Method B is the method of choice, since more concentrated solutions can be oxygenated and better spectra are generally obtained.

Reversible Oxygenation of Samples. Samples prepared by either of the above methods were removed from the vacuum line and shaken at room temperature until completely dissolved, and cooled to −79 °C in a dry ice/ethanol slush bath. A septum cap was placed in the bore of the EPR tube's o-ring joint, a small diameter exit needle was put through the septum, and the side arm was flushed for 2 min with O_2. The valve to the sample was then opened and the solution exposed to O_2 for 2 min, after which the valve was closed thus sealing the sample under 1 atm of O_2. The system was equilibrated by carefully tilting the tube. It is *very* important that the oxygenated samples not be allowed to warm to temperatures greater than −70 °C, in order to prevent excessive amounts of irreversible oxidation. Satisfactory EPR spectra can be obtained in the presence of small amounts of the irreversibly oxidized product, but if larger amounts are formed precipitation occurs and good spectra cannot be obtained. The reversible oxygenation is accompanied by a color change from green to golden-brown for the tetraarylporphyrin complexes, and a deepening of the red color for the octaethylporphyrin complex.

Preparation of the ^{17}O Samples. All ^{17}O samples were prepared by method B. After the addition of the solvent to the solid, the valve was sealed and the side arm fitted with a septum cap. After mixing at room temperature and cooling to −79 °C, the dead volume of the side arm was evacuated and back-filled five times with N_2 using a small gauge needle. The side arm was then evacuated and 3.0 mL of the ^{17}O-enriched O_2 was syringed into the dead volume using a gas-tight syringe. The valve was then opened and the system allowed to equilibrate for 2 min. The valve was finally sealed and the solution mixed as described above.

EPR Spectra. EPR spectra were observed on a Varian Associates E-4 spectrometer equipped with a Varian V-3400 9-in. magnet and a V-4533 X-band circular cavity. The microwave frequency was measured as described earlier.[15] Magnetic field calibration was checked with DPPH (g = 2.0037) and a F. W. Bell Model 660 digital gaussmeter. Spectra were taken at 77 K with the sample immersed in liquid nitrogen, at 4.2 K using liquid helium as refrigerant, or with the sample temperature maintained at approximately 10 K, constant to within ±0.02 K, using an Air Products Helitran Model LTD-310. The temperature stability at 10 K was determined with an uncalibrated Au/0.07% Au in Fe thermocouple. The four spin states of an S = 3/2 Mn(Por)(O_2) are split in zero field into two Kramers doublets (3/2, 1/2) (see below). The splitting for each Mn(Por)(O_2) was calculated from the known zero field separation (Δ) of MnTPP(O_2) and the EPR intensity (I) by the relationship

$$\frac{\Delta_{Mn(Por)(O_2)}}{\Delta_{Mn(TPP)(O_2)}} = \frac{\ln [I(3/2)/I(1/2)]_{Mn(Por)(O_2)}}{\ln [I(3/2)/I(1/2)]_{Mn(TPP)(O_2)}}$$

Computations. Computer calculations of EPR absorption spectra were done on a CDC 6600 using a modification of program EPR;[16] simulated spectra were calculated using program SIM14.[17]

Results

EPR spectra of Mn(TPP)(O_2) were obtained at liquid nitrogen (77 K) and liquid helium (4.2 K) temperatures, and at 10 K. Spectra of the other Mn[T(p-X)PP](O_2) adducts were taken at 77 and at 10 K. The Mn(OEP)(O_2) adduct behaved differently in that rapid spin-lattice relaxation at 77 K precluded observation of a spectrum at that temperature. However, the spectrum of this dioxygen adduct was readily obtained at temperatures below ~25 K.

A full spectrum of Mn(TPP)(O_2) has been presented previously;[1] the EPR spectra of the dioxygen adducts of all four of the porphyrins studied are qualitatively quite similar. The low-field regions of the EPR spectra of the four porphyrins studied, taken at ~10 K, are shown in Figure 1. Since the spectrum of Mn(TPP)(O_2) has already been described in some detail, only the essential features of the analysis will be presented.

The spectrum of Mn(Por)(O_2) is a superposition from two Kramers doublets with slight differences between doublets in at least the largest g value, g_1, and significant differences in the ^{55}Mn hyperfine splittings associated with this g value (Figure 2). That these two doublets belong to the same entity and are in thermal equilibrium is shown by the reversible changes in relative intensities as a function of temperature (Figure 2). From their unequal intensities (I), one can obtain the separation, Δ, between the upper and lower doublets: I(upper)/I(lower) = exp(−Δ/kT) (Figures 1 and 2). Because of the method of measurement, as described above, the values of Δ are determined relative to that of Mn(TPP)(O_2). These values are presented in Table I for the several Mn(Por)(O_2).

The spectra for the Mn(Por)(O_2) are interpretable in terms

Table I. Spin-Hamiltonian Parameters[a] for the Mn(Por)(O_2) Complexes

compd	Δ, cm^{-1} [b]	D, cm^{-1} [c]	E/D [d]	A, 10^{-4} cm^{-1} [e]	C, 10^{-4} cm^{-1} [e]
Mn(TPP)(O_2)	5.66 (1.0)	−2.46	0.3291	52.6	86.2
Mn[T(*p*-F)PP]-(O_2)	4.64 (0.82)	−2.02	0.3276	52.8	86.4
Mn[T(*p*-*n*-BuO)-PP](O_2)	5.06 (0.89)	−2.21	0.3221	53.6	86.4
Mn(OEP)(O_2)	7.44 (1.31)	−3.21	0.3427	52.2	88.1

[a] The parameters were calculated assuming $g_x = g_y = g_z = 1.995$. See text. [b] The number in parentheses is the value of Δ relative to that of Mn(TPP)(O_2), and is the direct result of experiment (see text). [c] Estimated error, ±0.07 cm^{-1}. [d] Estimated error, ±0.005. [e] Estimated error, $\pm 0.5 \times 10^{-4}$ cm^{-1}.

of an $S = 3/2$ system described by the spin Hamiltonian

$$\mathcal{H} = \beta_e[g_x H_x S_x + g_y H_y S_y + g_z H_z S_z] + D[(S_z^2 - 5/4) + \lambda(S_x^2 - S_y^2)] + [AS_zI_z + BS_xI_x + CS_yI_y] \quad (1)$$

where λ is the ratio of rhombic (E) to tetragonal (D) zero-field splitting (zfs) parameters ($\lambda = E/D$) and g_i and A_i are the g and hyperfine tensor principal axis components. The coordinate system for the zfs tensor can always be chosen such that $0 \leq \lambda \leq 1/3$, with $\lambda = 0$ corresponding to axial and $\lambda = 1/3$ to purely rhombic symmetries.[18] At zero applied field the four states of the $S = 3/2$ manifold split into two Kramer's doublets with the energy separation given as[19]

$$\Delta = 2(D^2 + 3E^2)^{1/2} = 2|D|(1 + 3\lambda^2)^{1/2} \quad (2)$$

If $D < 0$, as is the case for Mn(TPP)(O_2),[1] the lower ($3/2$) doublet is primarily composed of the $M_s = \pm 3/2$ states, the upper ($1/2$) doublet the $M_s = \pm 1/2$ states. In the Mn(Por)(O_2) systems, Δ is much larger than the X-band microwave quantum, so that only intradoublet transitions are observed at the accessible magnetic fields, and the two doublets act as independent EPR-active systems, each with effective spin of $S' = 1/2$ (EPR transitions within the $3/2$ doublet become strongly allowed when λ is large). In this limit the two $S' = 1/2$ systems exhibit effective g tensors, $g^{3/2}$ and $g^{1/2}$, reported previously, which are functions of λ but independent of D.[1]

If we assume for the moment that in eq 3 of ref 1b, $g_z = g_y \simeq g_e$, then for $\lambda = 1/3$, $g_z^{3/2} = g_y^{1/2} \simeq 5.472$; as λ decreases from $1/3$, $g_z^{3/2}$ increases and $g_y^{1/2}$ decreases and λ can be calculated from eq 3 of ref 1b and the difference $(g_z^{3/2} - g_y^{1/2})$. Considering the two overlapping sets of peaks in the vicinity of $g = 5.4$ for Mn[T(*p*-X)PP]O_2, we therefore assign the higher effective g value $g_1^{l} = g_z^{3/2}$, the lower value as $g_1^{u} = g_y^{1/2}$, and the respective hyperfine splittings as $A_1^{l} = A$ and $A_1^{u} = C$. The assignment corresponds to $D < 0$. With the further assumption that $g_y = g_z = 1.995$ (vide infra), λ can be calculated from eq 3, ref 1b, and thence D from eq 1 above. Results for hyperfine and zero-field splitting tensor components are tabulated in Table I. It can be seen that for all three tetraarylporphyrin complexes, $\lambda \doteq 1/3$, and that the large hyperfine anisotropies ($\Delta A = |A| - |C|$) are equal. The values of D are not the same, but are comparable. Whether any significance should be attached to these variations in $|D|$ is uncertain; the only obvious correlation is that $|D|$ appears to decrease as the para substituent becomes a stronger σ acceptor.

With $\lambda < 1/3$, the larger g value in the vicinity of $g = 5.4$ is $g_z^{3/2}$. For Mn[T(*p*-X)PP]O_2 this is associated with the lower doublet and smaller resolved ^{55}Mn hfs. For Mn(OEP)(O_2), however, the feature near $g = 5.4$ associated with the lower doublet also corresponds to the smaller hfs, but is associated with the smaller g value. Because of the similarity in ^{55}Mn hfs, we also assign this feature to the z-axis direction of the spin Hamiltonian (eq 1), requiring for Mn(OEP)(O_2) that $\lambda \gtrsim 1/3$. Table I also presents λ and $|D|$ for this system calculated as noted above. The $|D|$ for the OEP complex is noticeably larger than for the tetraarylporphyrin complexes. This might be correlated with the σ-donor properties of the peripheral substituents, but another possibility, related to the degree of flexibility of the porphinato core, is discussed below. This alternative possibility is consistent with the fact that the hyperfine anisotropy, ΔA, for the OEP adduct (Table I) is also significantly larger than that for the tetraarylporphyrins.

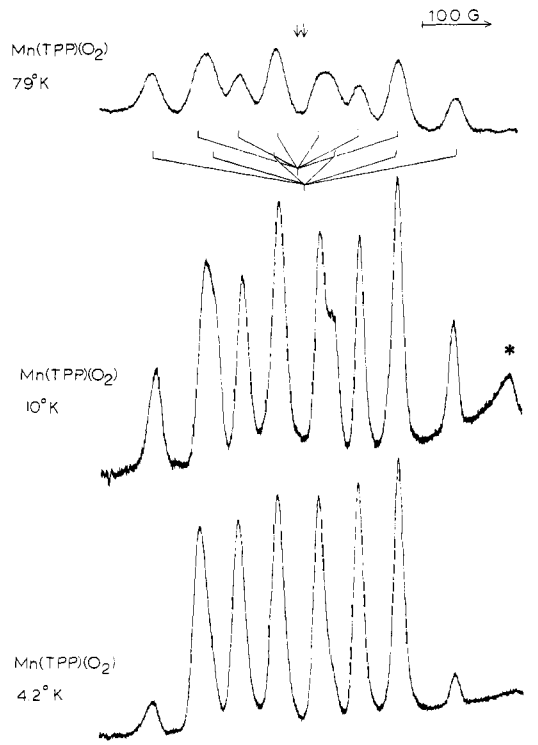

Figure 2. EPR spectra ($g = 5.4$ region) of Mn(TPP)(O_2) at temperatures of (A) 77 K; (B) 10 K; (C) 4.2 K. Asterisk indicates signal from rhombic iron in quartz.

Three comments regarding this analysis of the EPR spectra are appropriate. First, it is possible to rotate the zero-field splitting tensor for OEP to a "natural" coordinate system such that $\lambda < 1/3$; D in the new system would be positive, in apparent contrast to $D < 0$ for a tetraarylporphyrin in its natural system ($\lambda < 1/3$). However, for all four systems, $\lambda \doteq 1/3$, and by writing the zfs tensors in the form $(D_x S_x^2 + D_y S_y^2 + D_z S_z^2)$, it is easy to see that there is no physical significance to the apparent discrepancy in the sign of D when the zero field tensor for each porphyrin is in its "natural" system.

Second, the accuracy of the values of λ is to some extent dependent on the assumption that $g_y = g_z$. Actually either $\lambda \neq 1/3$ or $g_y \neq g_z$ will give rise to a difference in the effective g values of $g_z^{3/2}$ and $g_y^{1/2}$. For example, with $\lambda = 1/3$, the observed difference could be accounted for by g anisotropies of 0.008, 0.011, 0.022, and 0.018 for Mn(TPP)(O_2), Mn[T(*p*-F)PP](O_2), MnT[*p*-*n*BuO)PP](O_2), and Mn(OEP)(O_2), respectively. In general, these anisotropies are substantially larger than are observed for $S = 3/2$ ions, and so we ignore this potential complication and, as done previously,[1] take $g_z = g_{\perp} = 1.995$.

Finally, as stressed previously, the large values of the zero-field splittings, both $|D|$ and λ, and of the hyperfine anisotropy, ΔA, exhibited by the Mn(Por)(O_2) adducts are quite unusual for $S = 3/2$ metal ion systems. However, there is a quite recent EPR study of the linear triatomic molecule MnO_2, isolated in

an argon matrix.[20] This system also exhibits marked hyperfine anisotropy and has a value of D much closer to the values observed here than have most of the other d^3 systems reported. The properties of this triatomic were analyzed in terms of a d^3, $^4Mn(IV)$ ion, as we had done for $Mn(TPP)(O_2)$.

^{17}O Experiments. Previous experiments with 50% ^{17}O-enriched O_2 coordinated to Mn(TPP) were performed at liquid nitrogen temperatures, and no effect was observed.[1] These ^{17}O experiments have been repeated, again using Mn(TPP). This time the EPR spectra were measured at 10 K because the resonances of the $^{16}O_2$ adducts near $g = 5.4$ have appreciably smaller line widths at this temperature; fwhm $\sim$ 25 G at 77 K vs. 15 G at 10 K.

The spectra in the vicinity of $g = 5.4$ were scanned with care, and no additional resonances appeared in the spectra of $Mn(TPP)(O_2)$ (50% enriched ^{17}O). However, the lines of the enriched samples showed an ^{17}O hyperfine broadening of 2-3 G as compared to the $^{16}O_2$ adduct. Such a small effect would in fact have been unobservable with the broader resonances observed at 77 °C. Similar effects were observed in the spectra of adducts of Mn(OEP) with ^{17}O enriched O_2.

In order to estimate the ^{17}O hfs constant causing the observed hyperfine broadening, individual lines of the high-field edge of the $g = 5.4$ region of the spectrum were computer simulated (Figure 3). The simulations assumed two O atoms with equal hyperfine couplings and a 50% probability of ^{17}O enrichment (i.e., 25%, $^{17}O^{17}O$; 50%, $^{17}O^{16}O$; 25%, $^{16}O^{16}O$). This corresponds to a symmetrically bonded, edge-on dioxygen. Two possible end-on bonded schemes have been considered, one with a single interacting O (50% ^{17}O) and one in which the two oxygen atoms interact unequally with the unpaired spin, as observed for $Co(TPP)(B)(O_2)$.[2] However, within the accuracy of the line-width measurement ($\sim\pm0.5$ G), these would not have yielded significantly different results.

Individual ^{55}Mn hyperfine lines separately associated with the y and the z axes of the spin Hamiltonian were simulated, since the first and third lines in Figure 3 arise only from a single orientation (a single doublet); the middle resonance in Figure 3 was not simulated because it consists of overlapping lines from the two orientations (doublets). Visual comparison between observed and calculated spectra leads to a result for the z axis (lower doublet) of $A(^{17}O) \simeq 2.8 \pm 0.5 \times 10^{-4}$ cm^{-1} and for the y axis $C(^{17}O) \simeq 2.3 \pm 0.5 \times 10^{-4}$ cm^{-1}.

The observed ^{17}O coupling can arise from interactions of the nucleus with spin density on oxygen, but will also include a contribution from the dipolar interaction with spin density on the metal center. Assuming that the total spin density resides on the Mn (as will be justified below) the latter interaction can be approximated by the classical formula for point dipoles[21]

$$A_D(\theta) = 2\left(\frac{hg_e g_n \beta_e \beta_n}{R^3}\right)\left(\frac{3\cos^2\theta - 1}{2}\right) \quad (3)$$

$$= 2A_D\left(\frac{3\cos^2\theta - 1}{2}\right)$$

where $\mathbf{R}$ is the metal ion oxygen atom vector, $R = |\mathbf{R}|$, and θ is the angle between $\mathbf{R}$ and the external field. If, for example, $\mathbf{R}$ coincides with the z axis of the ^{55}Mn hfs tensor, then the observed couplings are related to the local contribution as follows:

$$A(^{17}O) = A_z(^{17}O) + 2A_D \quad (4)$$

$$C(^{17}O) = A_y(^{17}O) - A_D$$

Since we do not know the relative signs of the hfs of eq 4, it is impossible to ascertain the exact values for the local ^{17}O contributions, $A_i(^{17}O)$. However, since choosing the reasonable value $R \sim 1.8$ Å gives $A_D \sim 0.5 \times 10^{-4}$ cm^{-1}, in discussions below it will be adequate to consider the local contributions to the ^{17}O hfs to be isotropic, with a magnitude, $a(^{17}O) \simeq 2.3 \times 10^{-4}$ cm^{-1} ($\sim$2.5 G).

^{14}N Splittings. As a control whose rationale is discussed below, we examined the ^{14}N hyperfine interaction from the axial nitrogenous base, pyridine, in the five-coordinate, high-spin ($S = 5/2$) complex, Mn(TPP)(py). As previously discussed,[1] the spectrum for this adduct, and for the other Mn(Por)(B), has $g_\perp \sim 6$, $g_\parallel \sim 2$, and is typical of a d^5, $S = 5/2$ system where the microwave quantum ($\tilde{\nu} \sim 0.3$ cm^{-1}) is less than the tetragonal zero-field splitting parameter[21] ($D \sim 0.55$ cm^{-1} [22]). The ^{55}Mn splittings are essentially isotropic and well resolved, but the ^{14}N hfs from an axial base is not resolved. We therefore measured the line widths of the individual ^{55}Mn hyperfine components at $g \sim 6$ for this complex ($\sim$36 G), and for the high-spin, base-free Mn(TPP) ($\sim$30 G). The additional line width of $\sim$6 G for the pentacoordinate complex can be attributed to hfs from ^{14}N. As a rough estimate, the hfs constant is equal to one-half ($\frac{1}{2}I$) the observed broadening, and is $\sim$3 G.

Odd-Electron Configurations for Mn(Por)(O_2). The observed hyperfine interactions with ^{55}Mn and ^{17}O provide a basis for discussing the possible odd-electron configurations for the quartet ($S = 3/2$), Mn(Por)(O_2). In this section we shall consider only the disposition of those electrons which influence the magnetic parameters. A later section will consider overall electronic configurations for those few odd-electron configurations which are found to be compatible with experiment. As notation we use $[d^m][(\pi^*)^s]$ where m and s are respectively the numbers of *unpaired* electrons in d orbitals on Mn and in π^* orbitals on O_2. More detailed descriptions will include a specification of the particular d orbitals occupied; frequently we find it useful to label the orbitals by the irreducible representation in octahedral symmetry (t_2,e), despite the low symmetry which actually obtains.

The first type of configuration to consider involves odd electron(s) on O_2. There are various $[d^2][\pi^1]$ quartet configurations which place an odd electron in an antibonding π orbital of dioxygen; one such was calculated to be the ground state by a particular ab initio technique.[6] Earlier, we also considered the rather artificial case of spin coupling between a high-spin $^6[d^5]$ metal ion and $^3[(\pi^*)^2]$ oxygen through a coupling Hamiltonian $H_c = JS^{Mn}S^{O_2}$, as well as coupling between $^5[d^4]$ and $^2[(\pi^*)^1]$ by the same Hamiltonian. The results of ^{17}O enrichment experiments reported in this paper unambiguously rule out such configurations.

The EPR of ^{17}O-enriched cobalt dioxygen adduct shows that a single odd electron in a π^* orbital on dioxygen gives a coupling constant of $A \simeq 60$-90 G[5]. In an $S = 3/2$, $[d^2][(\pi^*)^1]$ configuration the coupling would be reduced by $1/3$ (Wigner-Eckart theorem),[23] leading to the prediction $A(^{17}O) \simeq 20$-30 G for this case. However, we observe a line broadening upon ^{17}O substitution which corresponds to $a(^{17}O) \approx 2.5$ G. Thus, *if* the only source of hfs by ^{17}O were from spin density on O_2, then there could be a maximum of $\lesssim$10% of an odd electron in π^*. Since, as discussed below, other sources of hyperfine interaction exist, this estimate is indeed generous, and this configuration can be ruled out. Analogous comments can also be made for the spin-coupling models.

Thus, for practical purposes the unpaired spin may be considered to be localized in 3d orbitals on Mn and we need only consider the several $[d^3]$ configurations. As a result, the ^{55}Mn hfs may be interpreted in terms of the manganese electron-nuclear coupling parameter, $P = g_e g_{Mn} \beta_e \beta_n \langle r^{-3} \rangle_{3d}$ and the isotropic coupling a_i, sometimes written $a_i \equiv -PK$, through first-order perturbation theory, by considering the several configurations in which three unpaired electrons are distributed among the d orbitals which are appropriate to a rhombically distorted octahedron. Choosing a coordinate system with x and y bisecting the angle between porphyrin N atoms and assuming

Table II. Hyperfine Constants for Relevant (d^3) Configurations[a]

configuration	hfs equation
$(t_2)^3$	
(a): $[(x^2-y^2)^1(xz)^1(yz)^1]$	$A_z = P[+8b^2/21 - K]$ $A_x = A_y = P[-4b^2/21 - K]$
$(t_2)^2(z^2)^1$	
(b): $[x^2-y^2)^1(yz)^1(z^2)^1]^b$	$A_z = P[-4/21 - K]$ $A_x = A_y = P[+2/21 - K]$
(c): $[(xz)^1(yz)^1(z^2)^1]$	$A_z = P[+8a^2/21 - K]$ $A_x = A_y = P[-4a^2/21 - K]$
$(t_2)^2(xy)^1$	
(d): $[(xz)^1(yz)^1(xy)^1]$	$A_x = A_y = A_z$
(e): $[(x^2-y^2)^1(yz)^1(xy)^1]$	$A_z = P\left[-\frac{6}{21}\left(1-\frac{4}{3}b^2\right)-K\right]$ $A_x = P\left[-\frac{4b^2}{21}-K\right]$ $A_y = P\left[+\frac{6}{21}\left(1-\frac{2b^2}{3}\right)-K\right]$

[a] Wave functions, rhombic distortion parameter (b^2), and electron-nuclear hfs parameters (P and K) are defined in text. [b] The previous equations for this configuration (ref 1) are incorrect.

that O_2 lies in the xz plane gives as basis orbitals $xy = d_{xy}$, $z^2 = ad_{z^2} + bd_{x^2-y^2}$, $yz = d_{yz}$, and $xz = d_{xz}$, and $x^2 - y^2 = ad_{x^2-y} - bd_{z^2}$, where $a^2 + b^2 = 1$ and b^2 is an additional parameter measuring configuration interaction introduced by a rhombic distortion.[19,24] Table II presents the hfs formulas for those configurations of the form $[t_2^3]$ and $[(t_2)^2(e)^1]$; $[(t_2)^1(e)^2]$ is presumed to be too high in energy to consider. In applying these formulas the hyperfine couplings of $Mn(TPP)(O_2)$ will be employed for illustrative purpose. Results from data for any other porphyrin are qualitatively similar.

We previously discussed the "natural" treatment of the EPR data in terms of a $[t_2^3]$ configuration (Table II (a)). This appears to satisfactorily account for the absence of large ^{17}O hfs (also see below) and for the anisotropic ^{55}Mn hfs. Upon assigning $A(obsd) = A_z = -53 \times 10^{-4}$ cm^{-1} and $C = A_y = -82 \times 10^{-4}$ cm^{-1}, and considering the plausible range of values $180 \times 10^{-4} \lesssim P \lesssim 235 \times 10^{-4}$ cm^{-1},[23] the equations in Table II give the reasonable values $a_i = -72 \times 10^{-4}$ cm^{-1} and a large d-orbital mixing: $0.21 \lesssim b^2 \lesssim 0.27$. This configuration and the value of b^2 were also found to be consistent with the large values of $|D|$ and λ.[1] However, note that mixing of d_{z^2} and $d_{x^2-y^2}$ by a rhombic distortion can only occur if the $Mn-O_2$ plane does not intersect the porphyrin plane along an N-N vector. This is the reason for supposing above that O_2 lies in the xz plane; b^2 would necessarily be zero if $Mn(Por)(O_2)$ were to adopt the symmetric, edge-on O_2 geometry with dioxygen eclipsing two N atoms, as is found in $Ti(OEP)(O_2)$.[25]

The four appropriate $(t_2^2)(e^1)$ configurations and their associated ^{55}Mn hfs equations are also listed in Table II. We first consider the two $[(t_2)^2(z^2)^1]$ configurations. For $[(x^2 - y^2)^1(yz)^1(z^2)^1]$, Table II (b), assigning $C = A_x$ and $A = A_y$, we obtain $P = 105 \times 10^{-4}$ cm^{-1} and $a_i = -63 \times 10^{-4}$ cm^{-1}. This result is independent of b^2, the rhombic distortion, and thus imposes no requirement on the O_2 orientation. The value of a_i is reasonable in size and magnitude but the P is sufficiently low to cast some doubt on the utility of this configuration; for example, in the low-spin $Mn(TPP)(CN)(NO)$, $P \sim 175 \times 10^{-4}$ cm^{-1}.[26] However, extensive delocalization in $Mn(Por)(O_2)$ might supply an explanation for the reduced P and so this configuration cannot be dismissed from consideration, contrary to our original statement.[1]

For odd-electron configuration (c), $[(xz)^1(yz)^1(z^2)^1]$, the equations are given in Table II, again with the requirement that $a^2 > b^2$. In this case, assigning $A(obsd) = A_z = +53 \times 10^{-4}$ cm^{-1} and $C = A_y = -82 \times 10^{-4}$ cm^{-1}, one obtains $a_i = -37 \times 10^{-4}$ cm^{-1} and essentially pure d orbital ($b^2 \sim 0$) with $P \approx 240 \times 10^{-4}$ cm^{-1}. The value of a_i is perhaps low, P is now perhaps too big, and in any case it is doubtful that the large observed $|D|$ can occur without considerable mixing of d orbitals (finite b^2). Thus, the configuration is considered to be relatively unattractive.

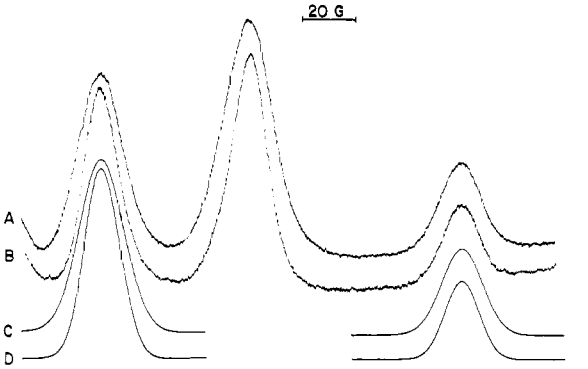

Figure 3. The three lines at the high-field edge of the $g = 5.4$ region of the 10 K EPR spectrum (see Figures 1 and 2) for (A) Mn(TPP) ($^{17}O_2$; 51.6 ^{17}O); (B) Mn(TPP)($^{16}O_2$); C and D are the best fit computer simulations of A and B, respectively, calculated as described in text.

These considerations of $[(t_2)^2(z^2)^1]$ make no reference to the geometry of the MnO_2 linkage. We feel, however, that considerations of the ^{17}O hfs provide convincing argument that the $Mn(Por)(O_2)$ do not adopt the bent end-on O_2 geometry with the manganese ion in either configuration (b) or (c). These two configurations place an odd electron in z^2, which must surely be strongly mixed with a filled σ-donor orbital on the oxygen atom directly bonded to manganese in this geometry. A very rough estimate of the ^{17}O hfs coupling to be anticipated can be obtained by considering Co(TPP)(L), in which the σ-orbital from a ligand L is also mixed with a half-filled metal z^2 orbital to give rise to hyperfine splitting, $A(L)$, from the coordinating atom of L. Consider first, $Co(TPP)(^{13}CO)$. The 2s and 2p spin densities on carbon are $\rho_s \sim \rho_p \sim 0.05$;[28] assuming equivalent mixing with ^{17}O in $Mn(TPP)(O_2)$, one would observe $a(^{17}O_2) \sim (1/2)\,(^{17}O a_{2s}/^{13}C a_{2s})(15\text{ G}) \sim 15$ G. Again the observed hfs is 10–20% of the value required for z^2 occupancy. In fact, the values are roughly what we might expect from the orbital mixing calculated for configuration (a), where $b^2 \sim 0.2$!

The above argument assumes comparable σ bonding by the d_{z^2} orbital on different metal ions in different spin states to the filled σ orbitals of different atoms. Fortunately, this broad assumption is susceptible to at least a partial experimental confirmation. If the bonding between d_{z^2} and a σ-donor orbital on ^{14}N is the same in the $S = 1/2$, Co(TPP)(py) as in the $S = 5/2$, Mn(TPP)(py), then the coupling constant in the high-spin compound should be $1/5$ that of the cobalt complex, or ~3 G. Nitrogen hfs are not resolved in Mn(TPP)(py), but should then contribute to the line width by about twice this ^{14}N coupling constant. In fact, we noted above that the individual ^{55}Mn hyperfine lines of Mn(TPP)(py) are, as expected, ~6–7 G broader than those we observed for base-free Mn(TPP).[22]

Extended Hückel calçulations of the end-on geometry support the occurrence of strong mixing between z^2 and the oxygen σ-donor orbitals.[27] What of the side-on geometry? Mixing between z^2 and the filled π orbital on O_2 is symmetry allowed in this case, but the calculations indicate that the degree of mixing is small.[27] Thus, the ^{17}O hfs results allow us considerable confidence in eliminating from further consideration the end-on geometry with a $[(t_2)^2(z^2)^1]$ configuration, but permit the side-on geometry.

It is perhaps worth emphasizing that the ab initio calculations, which erroneously favored a $(\pi^*)^1$ configuration, gave as the second-best alternative a $(z^2)^1$ configuration, and in both cases favored the end-on geometry.[6] The sources of the difficulties with these calculations will be discussed elsewhere.[22]

Of the two $[(t_2)^2(d_{xy})^1]$ configurations, (d) can be eliminated trivially because it predicts an isotropic ^{55}Mn hfs tensor, in disagreement with experiment. However, if we assign $A = A_x = -53 \times 10^{-4}$ cm^{-1} and $C = A_z = -82 \times 10^{-4}$ cm^{-1}, then the equations for $[(x^2-y^2)^1(d_{yz})^1(d_{xy})^1]$, Table II (e), give $a_i = -46 \times 10^{-}$ cm^{-1}; again taking $180 \times 10^{-4} \lesssim P \lesssim 235 \times 10^{-4}$ cm^{-1}, we get $0.2 \lesssim b^2 \lesssim 0.27$. Although a_i is somewhat small in magnitude, the configuration probably cannot be eliminated from consideration on this basis, and the range of values of b^2 is the same as that for (a). Finally, there is again no problem in accommodating the small ^{17}O hfs. Thus this configuration also appears to be consistent with the hfs data.

Discussion

The EPR results provide direct information about the odd-electron configuration of Mn(Por)(O_2). This in turn can be used to draw inferences regarding the geometry and total electronic structure of the adduct. However, before proceeding with this task, we discuss the information attainable from optical spectra. We originally noted that the spectra of Mn^{III}(Por)(X), where X is a bound anion, and Mn(Por)(O_2) are similar, suggest appreciable Mn $\rightarrow$ O_2 charge transfer.[1] Unfortunately, it appears that this fact cannot be used to draw conclusions regarding the detailed electron configuration of Mn(Por)(O_2).

In early studies of the high-spin Mn(III) porphyrin complexes, the "split-Soret" band they exhibited was viewed as most unusual.[29] However, this "hyperporphyrin" spectrum, as it is now called, is far more common than was first believed. It has been observed for a number of other metalloporphyrins with various d-electron configurations[30] and in particular is exhibited by the *low-spin* ($S = 1/2$) Mn(TPP)(CN)(NO) complex.[26] Thus, the similarity between spectra for Mn^{III}(Por)(X) and Mn(Por)(O_2) cannot reliably be used as evidence for a particular configuration, and we turn to considerations of the implications of the Mn(Por)(O_2) EPR results.

The simplest conclusion to draw from the EPR results is that the metal ion is displaced from the porphyrin plane toward dioxygen. Consider first the two permissible odd-electron configurations, Table II (a) and (e), which would involve all-electron configurations in which the z^2 orbital on manganese is unoccupied. In these cases there would be no electronic reason for a Mn(Por)(O_2) adduct with an in-plane manganese ion to refrain from binding a nitrogenous base as sixth axial ligand. The other permissible configuration, (b), is only possible with the edge-on geometry; this would sterically demand an out of plane manganese for effective Mn–dioxygen overlap and minimal O_2–porphyrin repulsion as in Ti(OEP)(O_2).[25]

The edge-on geometry is, as discussed earlier, consistent with the all-electron configuration which would most obviously correspond to the odd-electron configuration (a). If we extend the above notation to explicitly account for the five electrons from the parent $Mn^{II}(d^5)$ and the two electrons from parent $^3\Sigma$ dioxygen, we have $[(x^2-y^2)^1(xz)^1(yz)^1][(\pi_2^*)^4]$, with the electrons on dioxygen totally paired; this configuration corresponds to a peroxo-bonded high-spin d^3 Mn^{IV} ion. The actual extent of charge transfer would, of course, depend on the degree of mixing between d(Mn) and the accepting π^* orbital on O_2, as well as the amount of donation by O_2 through bonding between d(Mn) and the filled π orbital on O_2.

With the manganese ion out of plane toward an edge-on O_2, a slight "folding back" of the porphyrin ring from O_2 might explain the fact that $|D|$, which should increase with the rhombic distortion (b^2), is noticeably larger for Mn(OEP)(O_2) than for several para-substituted TPP derivatives. This difference is consistent with a greater deformation ("folding") of the more flexible OEP ring, as compared to the relatively more rigid TPP derivatives.[31] It might also be proposed that the large rhombic distortion arises from strong π bonding in a bent, end-on O_2 geometry; this, however, does not as obviously lead to an explanation of the variation of magnetic parameters with porphyrin.

Considering odd-electron configurations (b) and (e), the occurrence of two unpaired t_2 electrons would presumably come about because of strong bonding interactions between d_{xz} and one of the π^* orbitals on O_2. If the π^* orbital lies below d_{xz} in an MO interaction diagram, then an electron pair would fill a bonding orbital which is primarily dioxygen in character, while the predominantly d-like antibonding partner remained empty. Either configuration again leads to a formal valency of $Mn^{IV}(O_2^{2-})$.

However, configuration (e) requires the half-filled in-plane e orbital, d_{xz}, to be lower in energy than the empty level which is primarily the out of plane d_{z^2} orbital. This ordering is to be expected in six-coordinate complexes, but is *not* expected in a five-coordinate complex, either with the metal in plane or, as we conclude obtains here, with the metal out of plane;[32] this argument, which is supported by extended Hückel calculations,[27] leads us to dismiss (e). Thus, the only alternative to (a) appears to be a symmetrically bonded dioxygen with the odd-electron configuration (b).

Conclusions

Solely on the basis of the magnetic resonance parameters for the Mn(Por)(O_2) it has been possible to affirm the conclusion that the Mn ion is out of plane toward dioxygen and to rule out all but three odd-electron configurations, Table II (a), (b), and (e). Further consideration of orbital energies eliminates (e). Explicitly recognizing that formal valencies are not necessarily connected with charge distribtuions (e.g., in $(ClO_4)^-$, the *actual* charges on Cl and O are not +7 and −2, respectively), both configurations (a) and (b) can be assigned to the Mn^{IV}–O_2^{2-} valency. Analogy to other "peroxo" complexes[2] suggests the symmetric, edge-on geometry, and indeed our experiments indicate that configuration (b), which is favored by extended Hückel calculations,[27] could *only* obtain in this geometry.

Acknowledgments. This work has been supported by the National Science Foundation through Grant DMR 7601057 to the Northwestern University Materials Research Center, and by grants from the National Science Foundation and the National Institutes of Health.

References and Notes

(1) (a) Weschler, C. J.; Hoffman, B. M.; Basolo, F. *J. Am. Chem. Soc.* **1975**, *97*, 5278–5280. (b) Hoffman, B. M.; Weschler, C. J.; Basolo, F. *ibid.* **1976**, *98*, 5473–5482.
(2) (a) Vaska, L. *Acc. Chem. Res.* **1976**, *9*, 175–191, and references cited therein. (b) Basolo, F.; Hoffman, B. M.; Ibers, J. A. *ibid.* **1975**, *8*, 384–392, and references cited therein.
(3) Cheung, S. K.; Grimes, C. J.; Wong, J.; Reed, C. A. *J. Am. Chem. Soc.* **1976**, *98*, 5028–5030.
(4) (a) Jones, R. D.; Summerville, D. A.; Basolo, F. *J. Am. Chem. Soc.*, in press. (b) Szymanski, T.; Basolo, F. To be published.
(5) (a) Vansant, E. F.; Lunsford, J. H. *Adv. Chem. Ser.* **1973**, *No. 121*, 441–447. (b) Gupta, R. K.; Mildvan, A. S.; Yonetani, T.; Srivastava, T. S. *Biochem. Biophys. Res. Commun.* **1975**, *67*, 1005–1012.
(6) Dedieu, A.; Rohmer, M. M. *J. Am. Chem. Soc.* **1977**, *99*, 8050–8051.
(7) Shriver, D. F. "The Manipulation of Air Sensitive Compounds," McGraw-Hill: New York, N.Y., 1969.
(8) Adler, D. A.; Longo, F. R.; Finarelli, J. D.; Goldmacher, J.; Assour, J.; Korsakoff, L. *J. Org. Chem.* **1967**, *32*, 476.
(9) (a) Barnett, G. H.; Hudson, M. F.; Smith, K. M. *Tetrahedron Lett.* **1973**, 2887–2888. (b) Barnett, S. H.; Hudson, M. F.; Smith, K. M. *J. Chem. Soc.*,

Perkin Trans. 1 **1975**, 1401–1403.
(10) (a) Triebs, A.; Haberle, N. *Justus Liebigs Ann. Chem.* **1968**, *718*, 183–207. (b) Badger, M.; Jones, R. A.; Laslett, R. L. *Aust. J. Chem.* **1964**, *17*, 1028–1035.
(11) Boucher, L. J. *J. Am. Chem. Soc.* **1970**, *92*, 2725–2730.
(12) Adler, A. D.; Longo, F. R.; Kampas, F.; Kim, J. *J. Inorg. Nucl. Chem.* **1970**, *32*, 2443–2445.
(13) Buchler, J. H.; Eikelmann, G.; Puppe, L.; Rohbock, K.; Schneehage, H. H.; Weck, D. *Justus Liebigs Ann. Chem.* **1971**, *745*, 131–151.
(14) Kobayashi, H.; Yanagawa, Y. *Bull. Chem. Soc. Jpn*, **1972**, *45*, 450–456.
(15) Summerville, D. A.; Jones, R. D.; Hoffman, B. M.; Basolo, F. *J. Am. Chem. Soc.* **1977**, *99*, 8195–8202.
(16) Gladney, J. D.; Swalen, H. M. Quantum Chemistry Program Exchange, No. 134, Indiana University, Bloomington, Ind.
(17) Lozos, G. P.; Hoffman, B. M.; Franz, C. G. Quantum Chemistry Program Exchange, No. 265, Indiana University, Bloomington, Ind.
(18) Blumberg, W. E. In "Magnetic Resonance in Biological Systems", Ehrenberg, A.; Malmström, B. G.; Vänngard, T., Ed.; Pergamon Press: Braunschweig, 1967; pp 119–133.
(19) McGarvey, B. R. *Transition Met. Chem.* **1967**, *3*, 89–200.
(20) Ferrante, R. F.; Wilerson, J. L.; Graham, W. R. M.; Weltner, W. Jr. *J. Chem. Phys.* **1977**, *67*, 5904–5913.
(21) Wertz, J. E.; Bolton, J. R. "Electron Spin Resonance, Elementary Theory and Practical Applications", McGraw-Hill: New York, N.Y., 1972, pp 140–143.
(22) Hoffman, B. M.; Mahoney, D., unpublished.
(23) Abragam, A.; Bleaney, B. "Electron Paramagnetic Resonance of Transition Metal Ions", Oxford University Press: London, 1970.
(24) McGarvey, B. R. *J. Chem. Phys.* **1964**, *41*, 3473–3758.
(25) Guilard, R.; Latour, J.; Lecomte, C.; Marchon, J.; Protas, J.; Ripoll, D. *Inorg. Chem.* **1978**, *17*, 1228–1237.
(26) Wayland, B. B.; Olson, L. W.; Siddiqui, Z. U. *J. Am. Chem. Soc.* **1976**, *98*, 94–98.
(27) Hansen, L. K.; Hoffman, B. M. In progress.
(28) Wayland, B. B.; Minkiewicz, J. V.; Abd-Elmageed, M. E. *J. Am. Chem. Soc.* **1974**, *96*, 2795–2801.
(29) Boucher, L. J. *Coord. Chem. Rev.* **1972**, *7*, 289–329.
(30) (a) Hanson, L. K.; Eaton, W. A.; Sligar, S. G.; Gunsalus, I. C.; Gouterman, M.; Connell, C. R. *J. Am. Chem. Soc.* **1976**, *98*, 2672–2674. (b) Chang, C. K.; Dolphin, D. *ibid.* **1975**, *97*, 5948–5950. (c) Dawson, J. H.; Trudell, J. R.; Barth, G.; Linder, R. E.; Bunnenberg, E.; Djerassi, C.; Gouterman, M.; Connell, C. R.; Sayer, P. *ibid.* **1977**, *99*, 641–642, and references cited therein.
(31) Hoard, J. L. *Ann. N.Y. Acad. Sci.* **1973**, *206*, 18–31.
(32) (a) Hoffman, R.; Chen, M. M. L.; Elian, M.; Rossi, A. R.; Mingos, D. M. P. *Inorg. Chem.* **1974**, *13*, 2666–2675. (b) Hanson, L. K. Personal communication.

Pulse Radiolysis Studies of Decacarbonyldimanganese(0) and Halopentacarbonylmanganese(I). The Pentacarbonylmanganese(0) Radical

William L. Waltz,*[1] Ortfried Hackelberg, Leon M. Dorfman,* and Andrew Wojcicki*

Contribution from the Department of Chemistry, The Ohio State University, Columbus, Ohio 43210. *Received May 15, 1978*

Abstract: The pulse radiolysis of $Mn_2(CO)_{10}$, $Mn(CO)_5Br$, and $Mn(CO)_5I$ in ethanol solution has been investigated. The $Mn(CO)_5\cdot$ radical, which was observed, exhibits an optical absorption band with a maximum at 830 nm and a molar absorption coefficient of $\epsilon_{830} = 800 \pm 80\ M^{-1}\ cm^{-1}$. Absolute rate constants were determined for the reactions of the solvated electron with $Mn_2(CO)_{10}$ ($9.1 \times 10^9\ M^{-1}\ s^{-1}$), $Mn(CO)_5Br$ ($1.0 \times 10^{10}\ M^{-1}\ s^{-1}$), and $Mn(CO)_5I$ ($1.02 \times 10^{10}\ M^{-1}\ s^{-1}$). For the iodide system, $Mn(CO)_5\cdot$ is also formed by the reaction of α-ethanol radical with $Mn(CO)_5I$ ($1.5 \times 10^8\ M^{-1}\ s^{-1}$). The recombination of $Mn(CO)_5\cdot$ has a rate constant of $2k = 1.2 \times 10^9\ M^{-1}\ s^{-1}$; $Mn_2(CO)_{10}$ is identified as a final product in the radiolysis of the halide complexes. $Mn(CO)_5\cdot$ reacts with O_2 ($1.8 \times 10^9\ M^{-1}\ s^{-1}$).

Introduction

Organotransition metal radicals represent a rapidly growing class of reactive intermediates.[2-7] They have been encountered, on numerous occasions, in chemical reactions leading to the formation and/or cleavage of metal–carbon, metal–hydrogen, and metal–metal bonds. A number of them have been implicated in catalysis by transition metal complexes.[8] Yet, recent developments notwithstanding, relatively little is known about their structure, spectroscopic properties, and elementary reactions.

A severe limitation on continued rapid progress in this field is the paucity of general methods of production and direct observation of such transient species in solution.[9] At present, transition metal centered radicals have been best generated by conventional photochemical or flash photolytic cleavage of metal–metal bonds in metal carbonyl complexes.[5-7,11-14]

$$L_n(CO)_mM\text{-}M(CO)_mL_n \xrightarrow{h\nu} 2L_n(CO)_mM\cdot \qquad (1)$$

In these processes homolysis of the metal–metal bond is thought to occur via a σ(M–M) to σ^*(M–M) one-electron excitation.[15] The resultant short-lived radicals have been characterized indirectly either by spin trapping with nitroso compounds or by scavenging in halogen abstraction reaction with organic halides. Organotransition metal radical pathways have also been diagnosed by the observation of chemically induced dynamic nuclear polarization[16,17] and, less directly, by various methods of kinetic and stereochemical origin.[2]

The pulse radiolysis method[18,19] potentially represents a powerful and versatile alternative method to flash photolysis for the direct study of organotransition metal radicals in solution. Surprisingly, it has received little application toward these ends.[20] Attachment of the solvated electron to an appropriate organotransition metal compound is expected to produce a radical anion

$$L_nMX + e^-_{sol} \rightarrow L_nMX^- \qquad (2)$$

which may then undergo dissociation to generate a stable anion and the desired metal-centered radical.

$$L_nMX^- \rightarrow L_nM\cdot + X^- \qquad (3)$$

The present work was undertaken in a new program concerned with the application of pulse radiolytic methods to studies on a submicrosecond time scale of organotransition metal transients. The manganese carbonyls $Mn_2(CO)_{10}$ and $Mn(CO)_5X$ (X = Br, I) selected for this initial investigation represent two general classes of metal carbonyl compounds,

0002-7863/78/1500-7259$01.00/0